Plasma-modified wood sawdust waste for the removal of reactive blue II anionic dye from aqueous solution

Hortence Kameni, Moise Fouodjouo, Wilfrid Zé, Hussam Aldoori, Chems-Eddine Gherdaoui, Philippe Supiot, Ulrich Maschke, Samuel Laminsi

Plasma-modified wood sawdust waste for the removal of reactive blue II anionic dye from aqueous solution

Resíduos de serragem de madeira modificada por plasma para a remoção do corante aniônico reactive blue II da solução aquosa

DOI:10.34117/bjdv9n2-098

Recebimento dos originais: 17/01/2023
Aceitação para publicação: 16/02/2023

Hortence Kameni
Master of Mineral Chemistry
Institution: University of Lille
Address: Centrale Lille, UMR 8207-UMET, F-59000, Lille, France
E-mail: hortykameni@yahoo.fr

Moise Fouodjouo
PhD in Inorganic Chemistry
Institution: University of Yaoundé I, Laboratory of Applied Physical and Analytical Chemistry
Address: P.O. Box 812, Yaoundé Cameroon
E-mail: fouodjouomoses@gmail.com

Wilfrid Zé
Master of Chemical Engineering
Institution: University of Ngaoundéré, National Advanced School of Agro-Industrial Sciences
Address: P.O. Box: 454, Ngaoundéré, Cameroon
E-mail: zewilfried@yahoo.fr

Hussam Aldoori
PhD in Material Chemistry
Institution: University of Lille – Unité Matériaux et Transformations (CNRS – INRAE - UMET)
Address: 26, Rue de la Course, 67000, Strasbourg
E-mail: hussam.aldoori.et@univ-lille.fr

Chems Eddine Gherdaoui
PhD in Chemistry
Institution: Maxei Group
Address: 170, Allée de France-Zac, Artoipole-BP-22004-62060, arras Cedex9, France
E-mail: chemseddine.gherdaoui@maxei.fr

Philippe Supiot
PhD in Spectrochemistry
Institution: University of Lille
Address: Centrale Lille, UMR 8207, Lille, France
E-mail: philippe.supiot@univ-lille.fr

Ulrich Maschke
PhD in Material Chemistry
Institution: University of Lille
Address: Centrale Lille, UMR 8207-UMET, F-59000 Lille, France
E-mail: ulrich.maschke@univ-lille.fr

Samuel Laminsi
PhD in Mineral Chemistry
Institution: University of Yaoundé I, Laboratory of Applied Physical and Analytical Chemistry
Address: P.O. Box 812, Yaoundé Cameroon
E-mail: s.laminsi@yahoo.fr

ABSTRACT
The Removal of an anionic Reactive Blue 2 (RB2) dye in an aqueous solution was successfully achieved using a plasma-modified agricultural biomaterial waste. Sawdust from Moabi (Baillonellatoxisperma) and Sapelli (Entandrophragmacylindricum) was modified using non-thermal gliding arc plasma. The natural raw materials and plasma treated were characterized by Infrared Spectroscopy (FTIR), Thermogravimetric Analysis (TGA), Scanning Electron Microscopy (SEM), XRD, Chemical analysis by Fluorescence, Sorption Analyser, and Zetametry. Experimental parameters such as initial pH, contact time, adsorbent dose, initial RB2 concentration, and temperature were optimized. The results showed that the removal of Reactive Blue 2 dye was favorable at acidic pH conditions with the maximum capacity going from 172,85 to 200,91 $mg.g^{-1}$ to 98,19 and 149,02 $mg.g^{-1}$ respectively for raw and plasma-treated Sapeli and Moabi. The Avrami fractional-order kinetic provided the best fit to the experiments data and the thermodynamic adsorption data of untreated (SSB and SMB) and plasma-treated (SSM and SMM) sawdust followed an exothermic process. This work demonstrated that non-thermal plasma modified wood sawdust can be a good alternative absorbent for the removal of dye pollutants from an aqueous solution.

Keywords: non-thermal plasma, wood sawdust, dyes, adsorption equilibrium, biosorbent.

RESUMO
A remoção de um corante aniônico reativo azul 2 (RB2) em uma solução aquosa foi realizada com sucesso utilizando um resíduo de biomaterial agrícola modificado por plasma. A serradura de Moabi (Baillonellatoxisperma) e Sapelli (Entandrophragmacylindricum) foi modificada usando plasma de arco não-térmico deslizante. As matérias-primas naturais e o plasma tratado foram caracterizados pela espectroscopia de infravermelho (FTIR), análise termogravimétrica (TGA), microscopia eletrônica de varredura (SEM), XRD, análise química por fluorescência, analisador de sorção e zetametria. Parâmetros experimentais como pH inicial, tempo de contato, dose adsorvente, concentração inicial de RB2, e temperatura foram otimizados. Os resultados mostraram que a remoção do corante Reactive Blue 2 foi favorável em condições de pH ácido com a capacidade máxima indo de 172,85 a 200,91 mg.g-1 a 98,19 e 149,02 mg.g-1 respectivamente para Sapeli e Moabi cru e tratado com plasma. A cinética de ordem fracionária Avrami forneceu o melhor ajuste aos dados dos experimentos e os dados de adsorção termodinâmica de serragem não tratada (SSB e SMB) e tratada com plasma (SSM e SMM) seguiram um processo exotérmico. Este trabalho demonstrou que a

serragem de madeira modificada por plasma não térmico pode ser uma boa alternativa absorvente para a remoção de poluentes de corantes de uma solução aquosa.

Palavras-chave: plasma não térmico, serragem de madeira, corantes, equilíbrio de adsorção, biosorbente.

1 INTRODUCTION

The contamination of water by dyes is becoming one of the major environmental concerns in the world. These dyes are used in several sectors of activity, notably in the cosmetics, leather, food dyeing and textile industries. Most often, the effluents discharged by these industries into the aquatic environment are sources of serious pollution problems [1]. The site of the discharged wastewater containing dyes cause the obstruction of light necessary for photosynthesis of aquatic plants, which reduces the growth of algae and leads to ecological imbalance in the aquatic ecosystem; in addition, these pollutants also have toxic and carcinogenic effects in humans [2, 3]

At a time when international community is seriously cornes about clean water, which is more and more polluted, rare and overexploited according to the report of the world water day of march 22, 2022, it is becoming more that urgent to build up green methods, efficient and inexpensive solutions for the 3.6 billions peoples in the world who nowaday do not always have access to modern methods of water treatment. Many scientists are paying close attention to this issue, in line with the increasingly stringent standards for toxic discharge. Therefore, simple and effective technologies for the removal of pollutants from wastewater are currently underway. Among the existing methods are microbiological treatment, photocatalysis, chemical oxidation, ozonation, electrochemical oxidation and the adsorption process [4-6]. Among these techniques, the adsorption process is often preferred due to its convenience and simplicity of implementation. The adsorption process using activated carbon for the removal of dyes and other toxic products from wastewater is widespread, but some disadvantages such as high production cost increasingly limit its effective implementation. Therefore, there is a need to find inexpensive and locally available alternative adsorbents for the removal of dyes from aqueous solutions. Thus, one of them may be the use of natural and modified agricultural waste (unused resources) as sorbents [7]. Many waste biomaterials have already been tested such as: mango seeds, sugarcane bagasse, Jatropha curcas and cocoa shell [_8-10]

In this paper, we report the biosorption characteristics of moabi and Sapelli sawdust, waste biomaterials; residual biomaterials for the removal of various textile dyes from an aqueous solution.

The moabi (Baillonella toxisperma) belongs to the class Sapotaceae. The heartwood and sapwood are well differentiated. The heartwood is more or less dark pinkish brown. The moabi contains quantities of benzene alcohol extract (7.35%) and water (3.75%) [11]. The whole tree is used in traditional African medicine, particularly in the Cameroonian pharmacopoeia. The bark is also used by pygmies and Bantus to make themselves invisible. The trunk is used in construction wood. Sapelli, Entandrophragma cylindricum (Meliaceae), is a heavily exploited hardwood lumber species found in the tropical forests of Africa. This species is classified as vulnerable in the IUCN Red List of Threatened Species and occurs at low densities. It is also one of the wood species found in abundance in Cameroonian forests [12]. It is a reddish-brown hardwood and classified as fairly durable and the trunk is used in construction timber.

Several studies have demonstrated the effectiveness of biomass-derived materials for several applications, including the treatment of liquid effluents containing various types of pollutants [13-16]. The attractiveness of these materials lies in their surface properties, texture, availability, and low cost [16]. However recent studies demonstrated that these raw materials should be improved before utilisation [16, 17]. This improvement can be achieved by different types of modifications: thermal, wet chemical, plasma treatment, etc [16-18]. The ultimate goal of these treatments is to modify the surface chemistry and the microstructure of the material and thus to modulate properties: Absorbability, roughness, reactivity, and porosity [16-18]. Literature reports [16, 19, 20], have demonstrated that alkaline treatment of Ayous, Juniper and olive kernel fiber tended to hydrolyse ester functions and convert carboxylic functions into carboxylates. In addition, Hem Lata et al, Martin-Lara et al. Zou et al [20- 22] also reported that the biomass of acid treatment indicated an increase in the concentration of acid sites (carboxyl groups) and, subsequently in the adsorption capacity. They also reported that acid-modified biomass had a lower zero charge point (pzc) due to dissociation of weakly acidic oxygen groups and that acid treatment could destroy several bonds in the aliphatic and aromatic species of the raw biomass. In addition, several studies have shown that biomass, the main source of carbonaceous material, can be thermally modified. The resulting carbonaceous material, commonly called activated carbon (AC), has a large surface area,

a high adsorption capacity, a microporous structure and a particular surface reactivity, although these high qualities depend on the precursor material, the operating conditions (temperature and pH) and the nature of the adsorbate [13, 15, 17].

Recently, non-thermal plasma technologies have received increased attention [23,24]. Due to their advantages over conventional surface modification techniques. These advantages are related to operating and capital costs for considerable efficiency, simplicity of implementation, and does not involve any threat to the environment.

The advent and development of plasma technology have also made it possible to improve the surfaces properties of biomass. Non-thermal plasma is a source of highly oxidizing (°OH, NO°, H_2O) and acidifying (HNO_2, HNO_3) agents [25, 26], which can react with the surface of the biomass and bring some modifications in their characteristics. Thus, several works [26-28], have reported that non-thermal modification of carbon-based plasma with O_2 as feed gas in dry atmosphere improved the adsorption capacity of adsorbent whereas the use of N_2 or Ar under the same conditions reduced the specific surface area and pore volume. In addition, the wood industries have produced billions of tons of sawdust and shavings that are usually destroyed by combustion or used as fuel for cooking, with consequences on the greenhouse effect due to the large amount of CO_2 released. Therefore, the valorization of these agricultural wastes as low-cost adsorbents is of great interest topic nowadays as well as it reduced the resulting direct pollution problem. However, the raw materials exhibiting low efficiency for the high scale application at various effluents, the surface properties modification was undeniable. In the present work, the non-thermal plasma technique in atmospheric ambient conditions was used for the modification of sawdust materials in aqueous medium. The removal capacity of the plasma modified Moabi sawdust (Baillonellatoxisperma) and Sapelli (Entandrophragmacylindricum) were evaluated on synthetic effluent of RB2 in aqueous solution used as model pollutant.

2 MATERIALS AND METHODS

2.1 SOLUTIONS AND REAGENTS

Deionized water was used for the preparation of all solutions. RB2 dye (lot: CP3628, CAS: 1236-82-7 $C_{47}H_{49}N_3NaO_7S_2$; 856.03 $g.mol^{-1}$), purchased from Sigma Aldrich was used. The dye with a maximum absorbance of 604 nm was used without any purification. The chemical structure of RB2 is shown in Fig. 1. No color change is

produced when this dye is dissolved from pH 1.0 to 10.0. Different concentrations were obtained from 25 and 400 mg.L^{-1}. To adjust the pH of the solutions, sodium hydroxide or hydrochloric acid (0.10 M) solutions were used. The pH of the solutions was measured with a JENWAY-350 pH meter. The different solutions were centrifuged using a Medias + Low SPEED centrifuge and the residual concentration of RB2 was determined using a CARY UV-visible spectrophotometer.

Fig.1: Chemical structure of Reactive Blue 2 (A), Schematic representation of the wood cell wall (B) [30], Structure of cellulose and monomer unit of anhydroglucopyranose (C).

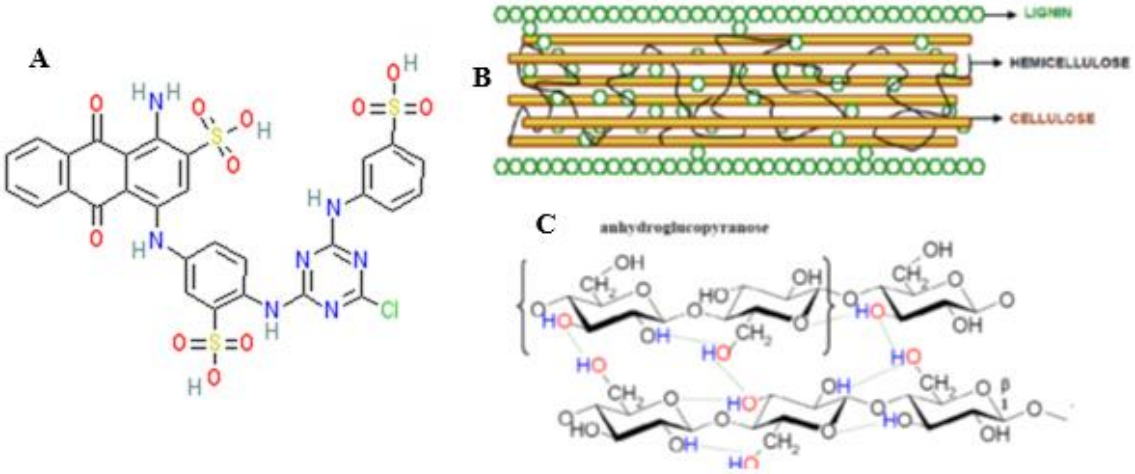

As we can see in Figure 1 (C) above, there are intramolecular and intermolecular hydrogen bonds that link the polymer chains to form microfibrils that alternate crystalline and amorphous zones. This crystalline structure combined with the high proportion of intramolecular hydrogen bonds makes cellulose à very stable compound [29 ; 30].

2.2 ADSORBENT PREPARATION

The study is carried out on sawdust samples from the species *Baillonellatoxisperma* (moabi) and (*Entandrophragmacylindricum*) Sapelli from the forests of Medoum (South Cameroon). The sawdust was collected in sawmill located in the industrial zone of the city of Yaounde. The material was sun dried for two weeks, then ground with an electric machine from the brand RETSCH. An electric sieve of the Fritsch brand was used to recover the wood fractions at 100µm according to our previous works. The quantification of the different proportions of the wood compounds of *Baillonellatoxisperma* and *Entandrophragmacylindricum* was carried out according to

protocols developed by the TAPPI standards (Technical Association of the Pulp and Industry) [31].

The raw sawdust was washed several times with tap water, then with distilled water, dried in the open air for 24 hours then in an oven at 80 ° C for 4 hours to remove the soluble water and particles adhering to the surface [16].

The extraction was performed using an organic solvent: ethanol / toluene mixture 1: 2 V/V with a volume V of 100 mL according to the protocols presented in previous works [9, 31]. The solvents are used to extract the largest amount of extractable. A 10g mass of sawdust was weighed in a cellulose cartridge and placed in the Soxhlet apparatus and soaked in 300 mL of organic solvents. The pre-extraction time was 4 to 6 hours. Finally, the sawdust in its cellulose cartridge was left under the high for 12 hours and dried in an oven at 70°C for 2 to 3 hours.

The plasma reactor used in these experiments is described by Czernichowski 2001[34].

The treatment is timed in minutes during the discharge.

Fig. 2: Schematic of the experimental setup involving a high voltage transformer (HV = 10 kV/1A in the open state; estimated 600 V/160 mA in working conditions); distance d = 2.5 cm between the electrode tips and the target. Gas flow rate: 800 L h^{-1}.

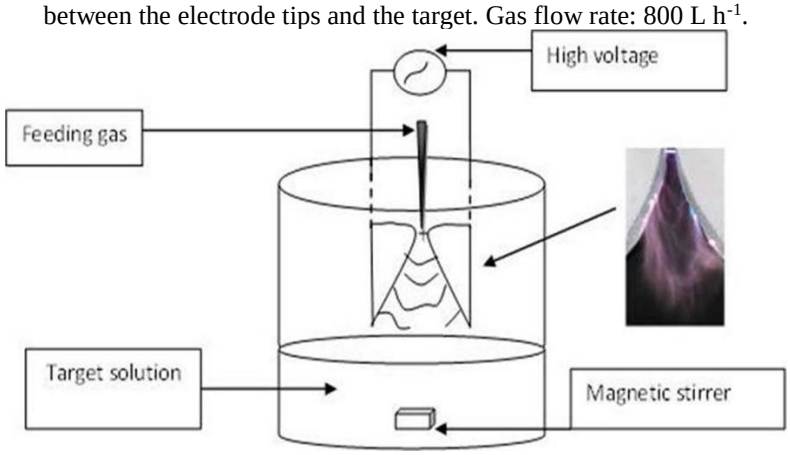

2.3 CHARACTERIZATION OF UNTREATED AND TREATED SAWDUST SAMPLES

To study the effect of polarization on the nature of surface chemical functions, the sawdust samples (Moabi and Sapelli) were characterized by Fourier transform infrared spectroscopy (FTIR) performed on a Perkin Elmer Frontier spectrometer. The sample was prepared as KBr pellets containing about 15% of the material. The analysis was performed over a wavelength range of 4000-400 cm^{-1} [9,18, 32]; thus, we obtained 12

accumulations for one spectrum. Chemical analysis by X-ray fluorescence was performed using an X-ray emission spectrometer using X Flash technology brand S2 RANGER BRUKER. The crystallinity index was determined using the empirical method of the height of the peak XRD [27, 33, 34]. The crystallinity index (CrI) was calculated from the ratio of the maximum height of 002 (I_{002}) and the height of the minimum value (I_{AM}: 2θ = 17 °). The calculation is performed using the equation (1) [39].

$$CrI = \frac{(I_{002} - I_{AM})}{I_{002}} \times 100 \quad (1)$$

The models are recorded in diffuse reflection mode using a D8 Advance BRUKER diffractometer equipped with monochromatic radiation CuKα anticathode (λ = 1.54056 Å) at 45 kV and 40 mA. The XRD patterns of powder samples were scanned with speed of 0.02°/0.5 seconds for 2θ values range from 5-60 °.

Thermogravimetry analysis (ATG / DTG), based on mass variation of a sample versus time or temperature under a controlled atmosphere. The device used is a Cahn optical microbalance type TG171. The heating rate was set at 10 ° C / min and the reference sample was alumina. The exothermic nature of phenomena can be appreciated from the derivative of ATG (DTG.

Scanning electron microscopy (SEM) was performed using the HITACHI TM-1000 equipped with an X-ray energy dispersive spectrometer (EDX), allowing the analysis of non-conductive samples. The sample to be analyzed is glued on a circular metallic sample holder, adaptable to the microscope's object holder, with a tungsten filament heated at 2700 K. The micrographs obtained allow to observe the microstructure of the sawdust surface and the effect of the non-thermal plasma treatment.

Isotherms were performed using a dynamic gravimetric water sorption analyzer from Surface Measurement Systems (DVS-Intrinsic). The sample was weighted using a digital microbalance (total capacity of 1 g; noise < 1µg). For this test, each sample had an initial mass of approximately 10 mg. The sorption cycles applied in this work started from zero percent relative humidity (RH) and the temperatures were 20°C and 40°C, respectively. Samples were maintained at a constant RH level until the weight change per min (dm/dt) value reached 0.0005% per min.

We used the electrophoresis technique to determine the zeta potential of different samples at various pH values. This technique measured, by optical means, the speed at which particles move under the action of an electric field. Therefore, the media must be sufficiently diluted (1% by mass) to allow the passage of light. Zeta potential measurements were performed on a Zeta Sizer Nano-ZS apparatus (Malvern Instruments), at room temperature with a solid/liquid ratio of 0.001 g/3 mL of distilled water. The suspension was equilibrated by shaking for 2 hat the initial pH.

2.4 ADSORPTION PROCEDURE

The adsorption experiments were performed in 50 mL flasks by mixing a constant amount of sawdust with a constant volume of aqueous RB2 solution. The flasks contents were homogenized by placing it in a shaker at 350 rpm for an appropriate time interval. The mixture was then centrifuged (4000rpm) and the residual RB2 in the supernatant liquid was determined by UV-Visible spectroscopy, as mentioned above. In the first set of experiments, the samples were triplicated and it was observed that there was 2% variability in the results. Therefore, it was not necessary to duplicate the experiments throughout the study. The adsorption per mg of adsorbent, q_e , and the percentage of RB2 adsorbed, % Removal, were calculated using equations (2) and (3) [8, 14], as follows:

$$q_e = \frac{(C_0 - C_e)}{m} V \qquad (2)$$

$$\%\,\mathrm{Re}\,moval = \frac{(C_0 - C_e)}{C_0} \times 100 \qquad (3)$$

Where q_e is the adsorption capacity (mg.g^{-1}), C_e and C_0 are the initial and equilibrium concentrations of RB2, respectively (expressed in mg. L^{-1}), m is the adsorbent dose (g) and V is the volume of the solution (mL).

2.5 ADSORPTION EQUILIBRIUM AND KINETICS STUDIES

The data from the essential biosorption experiments were analyzed using different isotherm models [14, 15, 17]: Langmuir Eq.(4), Freundlich Eq.(5), and Liu Eq.(6). Meanwhile kinetic models studied selected to analyze the data from the experiments are:

Pseudo-first-order (Eq. (7); Pseudo-second-order Eq.(8), and Avrami fractional model Eq. (9) [14, 15, 21, 22]

$$q_e = \frac{Q\max \times K_L \times C_e}{1 + K_L \times C_e} \quad (4)$$

$$q_e = K_F \times C_e^{1/nF} \quad (5)$$

$$q_e = \frac{Q\max \times (K_g \times C_e)^{nL}}{1 + (K_g \times C_e)^{nL}} \quad (6)$$

$$q_t = q_e \times \left[1 - \exp(-k_1 \times t)\right] \quad (7)$$

$$q_t = q_e - \frac{q_e}{\left[k_2(q_e) \times t + 1\right]} \quad (8)$$

$$q_t = q_e \times \left\{1 - \exp\left[-(k_{AV} \times t)\right]^{nAV}\right\} \quad (9)$$

Where q_e and $Q\max$ are the amounts of the RB2 dye adsorbed at equilibrium and adsorption capacities (mg/g), C_e is the equilibrium RB2 concentration in the solution (mg.L^{-1}) and K_L is the Langmuir constant (L.mol^{-1})., K_F (mg $^{(1-1/n)}$ L$^{1/n}$ g^{-1}) and n_F are the Freundlich equilibrium constants. K_g (L/mg) and n_L are the Liu equilibrium constants. q_t (mg/g) is amounts of the RB2 dye adsorbed at t (min), and k_1 is the rate constant of first-order adsorption (min^{-1}). k_2 is the rate constant of second-order equation (g.mg^{-1}·min^{-1}). t, k_{AV} and n_{AV} are the Avrami kinetic constant.

2.6 ADSORPTION THERMODYNAMICS

To describe the thermodynamic behavior of RB2 dye biosorption onto sawdust, thermodynamic parameters including the change in free energy (ΔG^0), enthalpy (ΔH^0) and entropy (ΔS^0) were calculated from the following equations [14]:

$$\Delta G^0 = \Delta H^0 - T\Delta S^0 \quad (10)$$

$$\log(\frac{q_e}{C_e}) = \frac{\Delta S^0}{2.303R} + \frac{-\Delta H}{2.303RT} \quad (11)$$

Where q_e (mg·g^{-1}) is the amount of metal ions adsorbed on the clay samples at equilibrium, C_e is the equilibrium concentration (mg·L^{-1}) and T is temperature in K and R is the gas constant (8.314 J·mol^{-1} ·K^{-1}). ΔG^0, ΔH^0 are expressed in kJ·mol^{-1} and ΔS^0 in kJ·mol^{-1} ·K^{-1} [49, 50].

3 RESULTS AND DISCUSSION

3.1 COMPOSITE MATERIAL CHARACTERIZATION

3.1.1 Infrared analysis (FTIR)

The change in surface groups that occurred during the non-thermal plasma treatment was analyzed by FTIR. The baseline has been corrected; they are not normalized; there are no contributions that have been made because of the questionable evolution of the processed peak that is isolated from the raw. Fig.3 showed the FTIR spectra of the SMB, SMM (a) and SSB, SSM (b) sawdust. It was observed an increase in intensity at 3401 cm^{-1} that could be attributed to an increase in the O─H bond stretching on the surface of the material after exposure to the plasma discharge. However, it is well-known that the gliding arc plasma is a source reactive species, especially HO$^{\circ}$ radical which can be fixed at the sawdust surface [9, 33, 34, 35]. In addition, we also noted an increase in the carbon of the polar carbonyl group C_6 and an oxidation of the primary alcohol leading to the formation of carboxyl (-COOH) as previously reported in the literature [9, 34, 36]. This functionalization of the fiber surface would enhance their hydrophilic property which is a key feature for the adsorption process. The main characteristic FTIR peaks of different samples and their comparison were gathered in table 1.

Fig. 3: Infrared analysis spectra (FTIR) of SMB, SMM (a) and SSB, SSM (b) sawdust and treated with plasma.

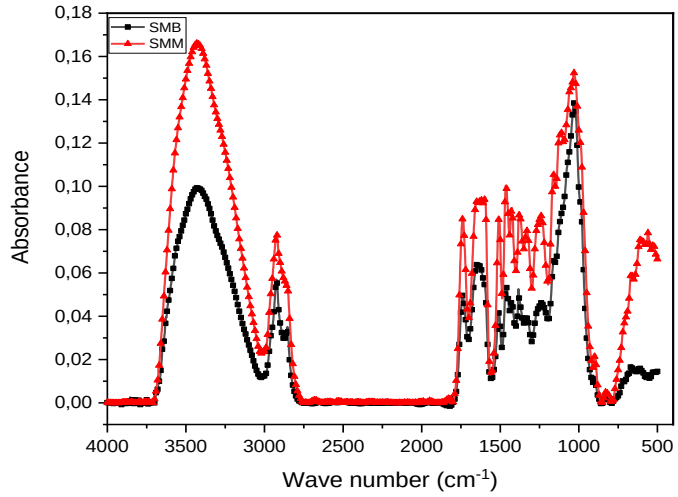

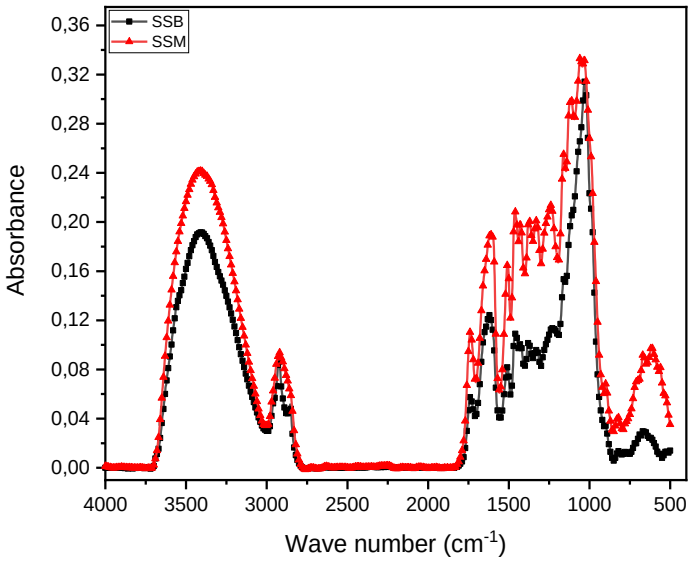

Table 1: Most relevant infrared bands of the SMB, SMM, SSB and SSM

FTIR (cm^{-1})	SMB	SSB	SMM	SSM	Peak characteristics
3570-3200	3401	3401	3411	3401	*O-Hbondstretching*
3000-2800	2921	2922	2925	2997	C-H stretch mode of the-CH3
1728	1700	1702	1704	1708	C= O stretch in C OOH
1650-1633	1634	1634	1634	1634	OH bending of adsorbed water
1515	1500	1488	1487	1557	C=C aromatic symmetrical stretching
1430	*1470*	*1460*	1762	1438	HCH and OCH in plane bending vibration

1372	1337	1337	1337	1374	C-H bending(deformation stretch)	+4
1320	1316	1316	1317	1319	C-H vibration in cellulose, hemicellulose, and lignin	-10
1261	1215	1215	1239	1237	C-O stretch vibration in lignin	-8
1042	**1035**	**1035**	**1036**	**1055**	**Asym, In-plane ring stretching modes**	**+1**

3.1.2 Chemical analysis: X-ray fluorescence

The chemical composition of sawdust samples was obtained by X-ray fluorescence analysis (Table 2). All the samples presented high content of the main mineral salts, such as calcium (CaO), potassium (K_2O), Silica (SiO_2), phosphorous (P_2O_5). The other elements are in trace with a percentage lower than 1%. The overall results showed that the chemical elements contained in sawdust samples were relatively similar with the exception of magnesium which is not present. However, the silica content practically doubled in the case of Sawdust from Sapelli compared to the content of Sawdust from Moabi. Depending on the percentage of oxides, the yield of synthetic products would be better for sawdust from Sapelli [36]. Non-thermal plasma does not affect the mineral composition (there is no inorganic change in the mass) of SMB, SMM and SSB, SSM. However Non-thermal plasma may oxidize some oxide present by increasing their oxidation number.

Table: 2 show the results of the chemical X-ray analysis of sawdust expressed in% of mass.

Major Composition	**CaO**	**SiO_2**	**P_2O_5**	**K_2O**	**SO_3**	**Fe_2O_3**	**Cl**	**CuO**	**BaO**	**ZnO**	**MgO**	**Total**
SMB	25,32	15,50	14,33	9,59	19,55	2,09	12,06	0,51	0,37	0,38	-	99,70
SMM	25,36	15,50	14,33	9,62	19,59	2,12	12,15	0,61	0,39	0,39	-	100,06
SSB	28,57	33,47	9,25	2,56	7,43	0,86	3,40	0,12	0,16	-	13,89	99 ,71
SSM	28,57	33,50	9,29	2,57	7,43	0,87	3,50	0,19	0,19	-	13,99	100.07

3.1.3 Crystallinity index (CrI) of sawdust from Moabi and Sapelli

The X-ray diffractograms of untreated and non-thermal plasma treated sawdust samples were depicted in Fig. 4. It can be seen that all samples exhibited cellulosic form, characteristic of native cellulose in lignocellulosic materials with a clear dominance of the beta I allomorph [29, 37]. The diffraction intensity increased for SSM and SMM compared to untreated sawdust samples due to the reduction of hemicelluloses upon treatment. Some authors investigated on the lignocellulosic materials surface modifications after plasma treatment and they reported an enhance of crystallinity with a record value 46.9% [33]. For these wood materials, once treated with plasma, the crystallinity index recorded were 74% and 66% for SMM and SSM sawdust treated with plasma respectively. However, it can be concluded that the action of plasma treatment is more effective on the amorphous parts of sawdust. As cellulose is the essential constituent of wood in a matrix of lignin and hemicellulose, the latter exists in several polymorphic states, that of the native cellulose which is cellulose I [38]. The peaks values at 14.9 °, 17 ° (I_{AM}) and 2θ = 22.7 ° (I_{002}) correspond to the diffractions of the (101), (110) and (002) planes, respectively, while the peaks at 14.9 ° , 22.7 ° , 34 ° correspond to (101) (002) and (004), planes of crystalline cellulose respectively[36, 39]. The X-ray spectra of the analyzed samples show crystalline peaks located in the (101), (101) space planes that were almost at the same positions and similar relative intensities. [39, 40, 41].

Fig. 4: X-ray diffraction diagram of SMB, SMM, SSB and SSM

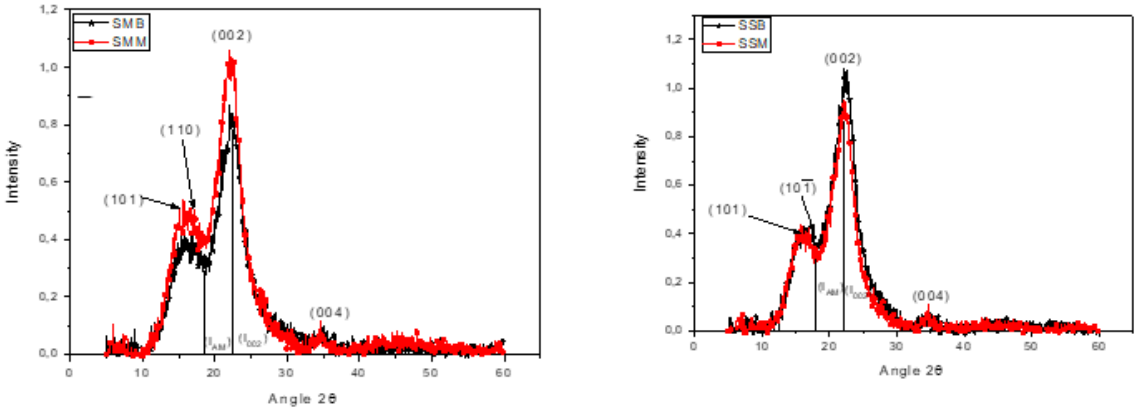

3.1.4 Thermogravimetric analysis (TGA/ DTG)

The results of thermogravimetric analysis for SMB, SMM, SSB and SSM are presented in Fig. 5. For SMB and SSB, the differential thermogravimetry (DTG) curves (Fig. 5a and 5c) show an intense peak at 40°C, corresponding to the release of free water

contained in the fibers 344 and 415°C for SMB, 340 and 430°C for SSB corresponding to the decomposition of organic matter contained in SMB and SSB [42]. The TGA curve shows that the mass losses can be divided into three stages. The first stage from 40 to 210 °C, with a mass loss of about 2.97%, for SMB, from 40 to 200 °C, with a mass loss of about 5.62%, for SSB that can be attributed to the removal of adsorbed water [42]; the second stage from 200 to 420°C with the maximum main peak (DTG) at 344 °C and a mass loss of 57, %. 57.4% for SMB, from 210 to 430°C with the maximum main peak (DTG) at 340°C and a mass loss of 60.39%. 60.39% for SSB is attributed to the decomposition of cellulose and hemicellulose [43]. The last stage from 385 to 700 °C, with a mass loss of about 38.6% and a very intense peak of (DTG) at 560°C, 560 °C, for SMB, from 400 to 700 °C, with a mass loss of about 33.99% and a very intense peak of (DTG) at 560°C, 560 °C, for SSB can be attributed to the decomposition of the residual carbonaceous backbone [8]**.**

In Fig. 5(b, d), the initial mass loss (about 9.5% and a maximum DTG peak at 60 °C) for SSM, (about 6.33% and a maximum DTG peak at 48 °C) for SMM are not significant. Maximum DTG peak at 80 °C) due to the release of adsorbed water molecules is greater than that of water molecules. This is due to the combined effects of densification and site activation (-OH groups) on the fiber surfaces by acidifying species such as NO° formed in aqueous solution during the gliding arc plasma treatment [24], which consequently readily bind water molecules (SSM and SMM). The other two peaks of the DTG curve (Fig. 5b and 5d) appear at 344 and 427 °C, with corresponding mass losses (TGA) of 60 and 34%, for SMM and at 340 and 420 °C with the corresponding mass loss(TGA) of 52.8 and 31.66%, for SSM, being attributed to the decomposition of cellulose and hemicellulose for the first and second phase of the process of cellulose and hemicellulose for the former and to lignin decomposition for the latter [44]. Indeed, the shoulder observed between 200 and 400 °C, for SSM and SMM, is attributed to the thermal decomposition of lignin and hemicellulose [45]. This indicates a reduction of these elements in the fiber after plasma treatment.

Fig. 5: Thermogravimetric curves (ATG / DTG) of sawdust from SMB (a), SMM (b), SSB(c) and SSM (d)

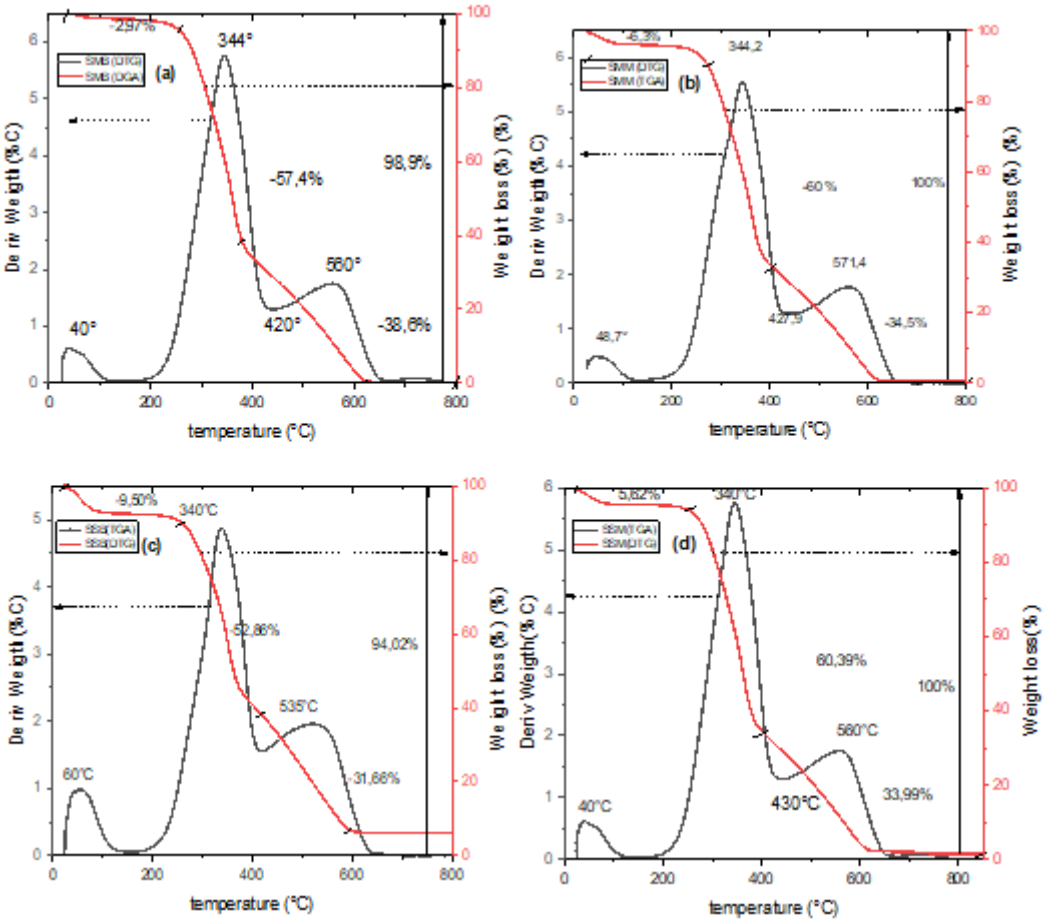

3.1.5 Scanning electron microscope (SEM) morphology

Fig.6 shows SEM micrographs of untreated (SMB) and plasma treated (SMM) Moabi sawdust (a-b) and untreated (SSB) and plasma treated Sapelli (SSM) (C-d). The shell does not disappear during plasma treatment; the image shown in fig.6 (c) and (d) revealed a more or less irregular outer surface of semi-heterogeneous structure of the SMM and SSM as well as the presence of intercellular voids in the form of partially observed circular cavities and porous structures. The lines of small holes observed in Fig. 6 (c) and 6 (d) called pits and the fibrous appearance observed in Fig. 6 (a) and 6 (b) allowed the exchange of substances with the cells making possible the adsorption process onto SMM and SSM surfaces. After non-thermal plasma treatment, cavities initially containing extractables encapsulated have been freed with bigger size. Likewise it is also observed that non-thermal plasma treatment deformed exterior ribs and the deteriorated the surfaces of SMM and SSM. This is due to the fact that reactive species (peroxides, anions and superoxides) generated during the plasma discharge act in the breakdown of

structurally important bonds of extractables [46]. As a result, there is separation of the cell layers and consequently the extravasation of essences and resins. The highly energetic plasma species collided with the external surface of Moabi and Sapelli and destroyed the original surface pore structure and produced new cavities [9, 29, 45, 47]. These modifications increase the affinity of the studied materials with chemical products.

Fig.6: SEM micrographs of SMB (a), SMM (b), SSB(c) and SSM (d)

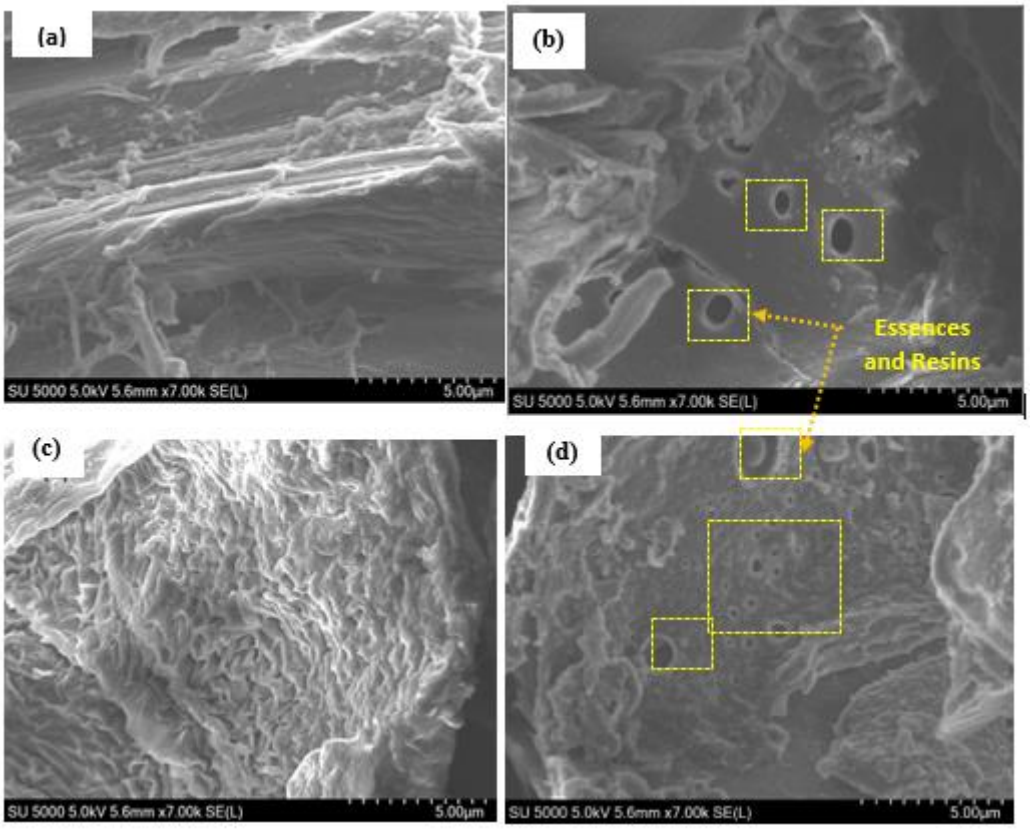

3.1.6 Isotherms of sorption

The experimental sorption isotherms of the studied biosorbents are presented in Fig.7a and 7b. They show a sigmoid shape which is characterized by a combination of hydrated water (monolayer of water molecules) and dissolved water (multilayer of water molecules). The shape of the sorption isotherm curves is typical of wood as has also been observed in the literature [1, 4, 14, 16]. For a given relative air humidity, as temperature increases, the equilibrium water content decreases. The effect of temperature on the sorption isotherms is quite small. The results are also consistent with those of [14]. They were obtained at 20°C and 40°C. However, sorption isotherms presented in the literature and obtained on some tropical woods indicate a slightly higher effect of temperature [48]. The extractives, cellulose, hemicelluloses and lignin contents of the studied woods are

different from those of the tropical woods presented in the previous studies. For a given relative humidity, the equilibrium moisture content is higher during the desorption phase than during the adsorption phase. Non-thermal plasma treatment affects the sorption isotherms (SMM and SSM) of Moabi and Sapelli. The adsorption and desorption isotherms of Sapelli (Fig. 7a) at 40°C show that the equilibrium water content decreases with relative humidity when exposed to non-thermal plasma (SSM). For Moabi sample (Fig. 7b), the evolution of the equilibrium water content is slightly affected during adsorption but for desorption the variation is more pronounced from 0 to 60% RH. Hence, the non-thermal plasma reduced the water content of the lignocellulosic material.

Fig. 7: Sorption isotherms of SSB, SSM (7a) and SMB, SMM (7b)

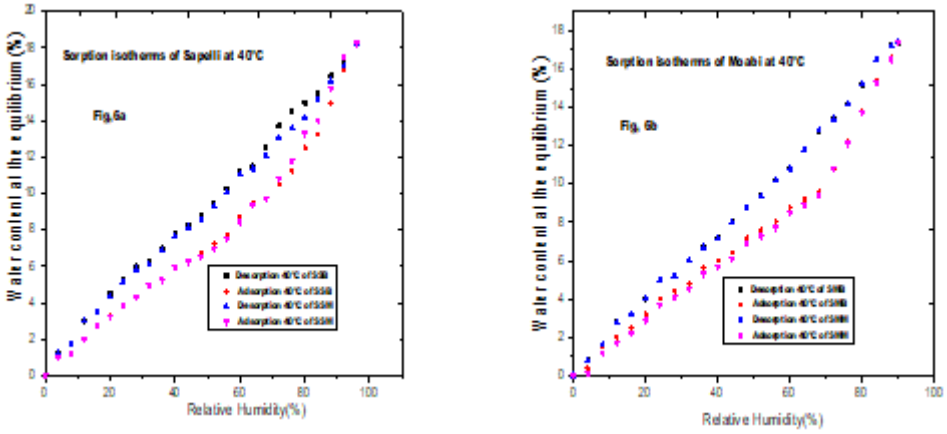

3.2 BATCH BIOSORPTION STUDIES

3.2.1 Zeta potential

Fig. 8 depicts the measurements of the Zeta potential of Moabi and Sapelli sawdust untreated (SSB and SMB) and plasma treated as a function of the initial pH.

The values of the zero point of charge of SMB, SMM, SSB and SSM were 2.60, 2.30, 1.85 and 170, respectively. Thus, for pH below the zero-charge point, the zeta potentials values were positive. Accordingly, the biomass surfaces were positively charged and can act as cations, whereas for pH above the zero charge point, the biomass overall surfaces were negatively charges and can easily retain cations. In this latter condition the charge of lignocellulosic materials is associated with carboxyl and phenolic groups -OH. [42, 49]

Fig. 8: Variation of zeta potential for SMB, SMM (a) and SSB, SSM (b) sawdust

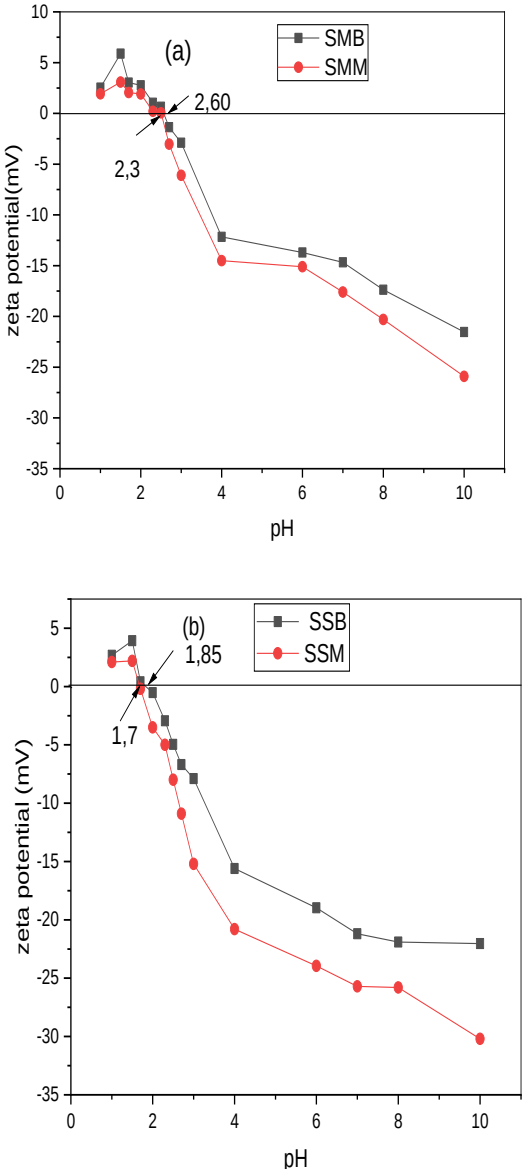

3.2.2 Effect of adsorbent dosage

To determine the adsorbent dosage for optimal adsorption on RB2 (Reactive blue 2) dye, 20 mL of RB2 solution was mixed with a given mass of adsorbent that varied from 0.0005 g to 0.5 g. The contact time was ninety min and the solution was stirred at 350 rpm. From Fig.8(a) (Supplementary material.), it can be seen that the amount of RB2 uptake using these adsorbents at equilibrium increases with the adsorbent dose. However, at the equilibrium, the sorption rate increases from 19.7 to 89.8, 19.9 to 95.6, 19.5to 76.0 and 24.5% to 89.6% for SSB, SSM, SMB and SMM respectively. This can be attributed to an increase in biosorbent concentration, which increased the available surface area and sorption sites [50].

3.2.3 Effect of Contact time

Fig .9 shows the evolution of the absorption amount of RB2 dye with the time of contact. The adsorption capacity of RB2 dye appeared to increase with time and reach equilibrium after 90, 50, 50 and 35 min for SMB, SMM, SSB and SSM, respectively. Adsorption is rapid and reaches a maximum after 30 min of contact, followed by a slight gradual increase over time until it reaches equilibrium. This may be because initially the surface adsorption sites were readily available [40].

Fig 9: Effect of the treatment time on the RB2 removal uptake. SMB, SMM (a) and SSB, SSM (b) : C_0=50mg/L, PH 1.0 Temperature was fixed at 298 K; biosorbent dosage1.5 g/ 500 mL for Sapelli and 2.5g/500mLfor Moabi.

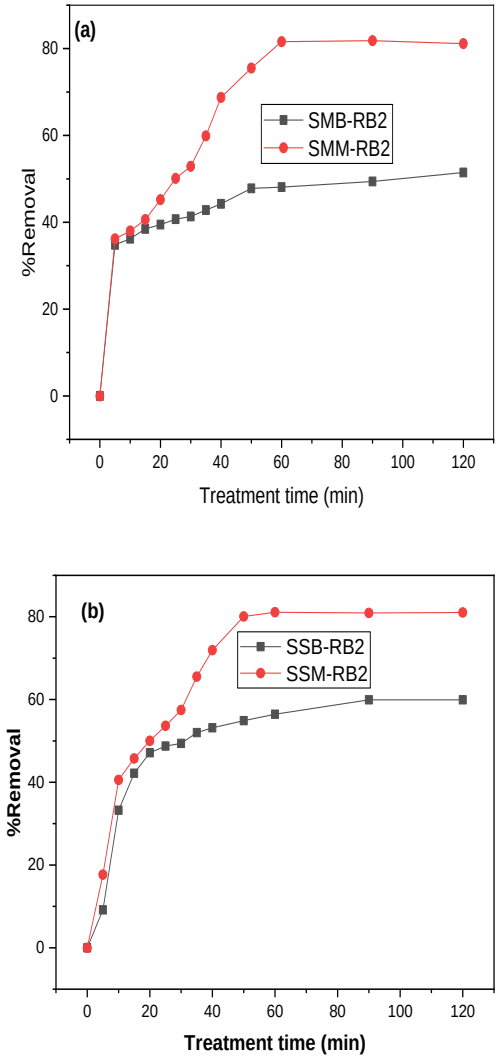

3.2.4 Effect of the initial PH of the dye solution on biosorption

The uptake and percent removal of dyes by biosorption from aqueous solution is strongly affected by the pH of the adsorbed solution [52, 53]. The effect of initial pH on

the removal of reactive blue 2 or RB2 (50 mg L^{-1}) using untreated Moabi sawdust (SMB) and Sapelli (SSB) and cold plasma treated Moabi sawdust (SMM) and Sapelli (SSM) was investigated in the pH range (1-10) and the adsorbent dose maintained at 1.25g / 500 Ml for SSB and SSM and 2.5g / 500 Ml for SMB and SMM. The results are shown in Fig.10 (10a and 10b). It was observed that for SSB and SSM sorbents, the percentage removal of RB2 decreases from 84.1 to 26.6%, and from 99.7 to 29.9 respectively and for SMB and SMM sorbents, the percentage removal of RB2 decreases from 82.0 to 21.8%, and from 98.6 to 27.9 respectively with the increase in pH. This was confirmed by the Zeta potential study (Fig. 8).

Fig. 10: Effect of pH on the biosorption of RB2 dye, using SMB, SMM (a) and SSB, SSM (b) biosorbents. Temperature was fixed at 298 K; mass of biosorbents 1.5 g/ 500 mL for SSB, SSM and 2.5g/500mLfor SMB , SMM; initial dye concentration at 50 mg L^{-1} of RB2.

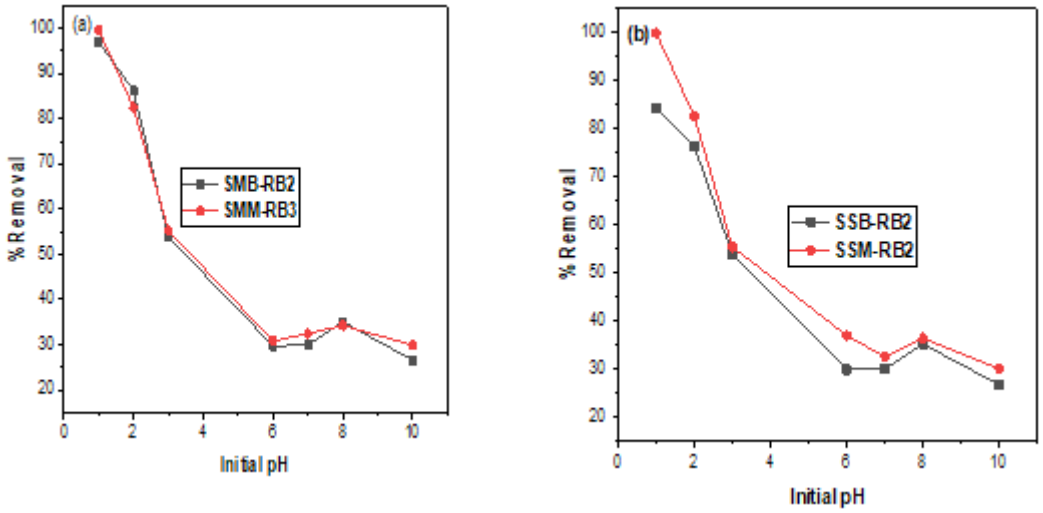

3.2.5 Effect of initial concentration

Fig. 11 shows the amount adsorbed relative to the initial concentration for an equilibrium time of 90, 50, 50, and 35 min for SMB, SMM, SSB, and SSM respectively. The amount of dye removed at equilibrium increased from 40.6 to 336.9 mg. g^{-1}, 46.4 to 416.0 mg. g^{-1}, 80.0 to 599.3, 85.9 to 630.0 mg. g^{-1} corresponding to SMB, SMM, SSB, and SSM respectively; with increasing RB2 dye concentration from 25 mg.L^{-1} to 400 mg.L^{-1}. It is clear that the removal of RB2 dye is dependent on the initial concentration. This may be due to the fact that the initial concentration of RB2 dye provides the strength to overcome the mass transfer resistance between the solution and the adsorbent [43].

Fig. 11: Influence of initial concentration (mass adsorbent SSB =SSM = 0.05 g mass adsorbent SMB =SMM = 0.1 g, pH = 1.0 ± 0.1, V = 20 mL, T = (293 ± 0.1) K, adsorption time = 120 min).

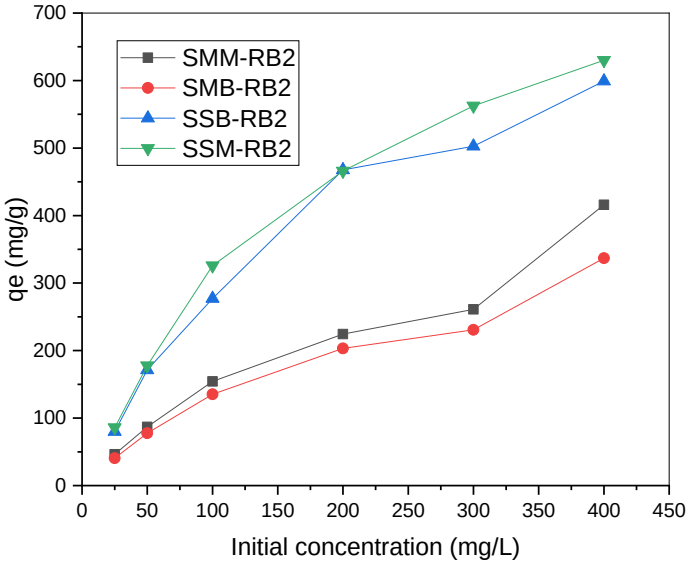

3.2.6 Equilibrium studies

Three isothermal models (Langmuir, Freundlich, and Liu) attempted to fit experimental data of RB2 adsorption on sawdust sorbents (SSB, SSM, SMB and SMM) and the results were depicted on Fig 12 The different isothermal modeling parameters calculated and the correlation coefficients (R^2) are shown in Table 3.

Fig. 12: Adsorption isotherms of RB2 adsorption onto SSM (a), SSB (b) SMB©, and SMM (d) ($m_{adsorbent}$ SMB, SMM = 0.1 g, ($m_{adsorbent}$SSB, SSM=0.05 T = (293 ± 0.1) K, pH = 1.0 ± 0.1.))

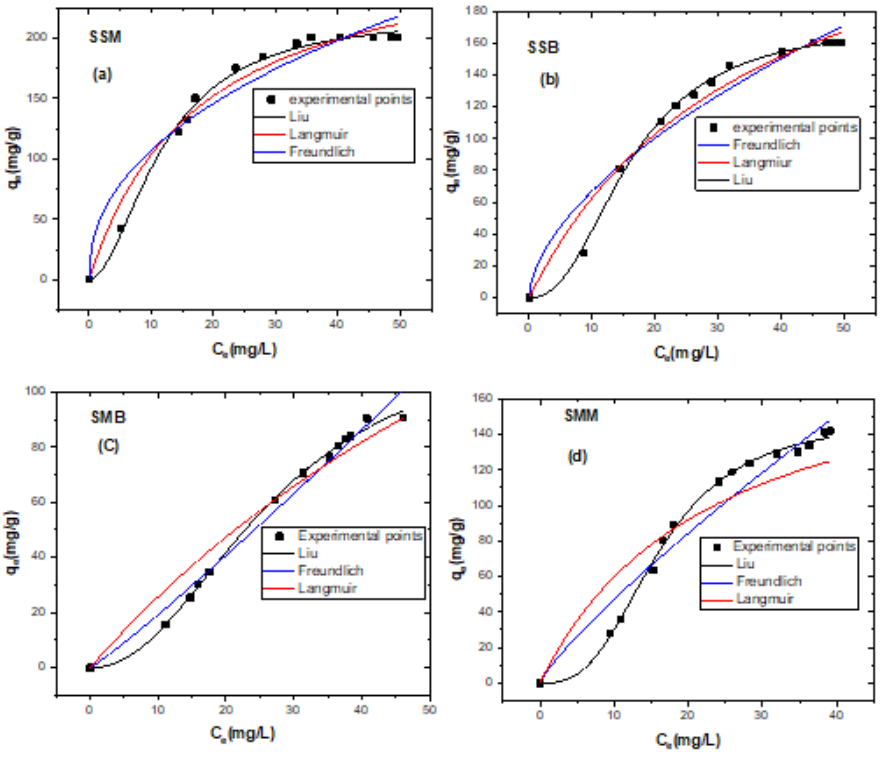

Table3. Kinetic parameters for RB-2 removal using SMB, SMM, SSB and SSM as biosorbents

Isotherms	SSB	SSM	SMB	SMM
Langmuir				
q_{max}(mg.g^{-1})	160.68	200.02.	86.28	140.2
K_L (L.mg^{-1})	0.0278	0.0565	0.0093	0.0426
R^2	0.9663	0.9766	0.9546	0.8804
Freundlich				
n_f	1.7176	2.2622	0.9225	1.1915
K_f	17.556	38.821	1.5828	6.8301
R^2	0.9435	0.9396	0.9830	0.9512
Liu				
Qmax (mg/g)	172.85	200.91	98.19	149.02
K_g(L/mg)	0.0620	0.0841	0.0367	0.0620
R^2	**0.9974**	**0.9942**	**0.9978**	**0.9982**

Conditions: temperature was fixed at 293 K; contact time, pH, and biosorbent dosage were fixed at 90 min, 1.0 and 2.5g/500ml; 50 min, 1.0 and 2.5g/500ml; 50 min, 1.0 and 1.5 g/ 500 mL; 35 min, 1.0 and 1.5 g/ 500 mL for SMB, SMM, SSB and SSM, respectively. From the modeling results, it can be observed that the Liu model seems to be the most fitted.

In this study, the n_f values of the Freundlich model are greater than one in all cases and show that the biosorption is quietly favorable [53]. According to Langmuir's isothermal model, the maximum amounts of dyes adsorbed were 13.3, 38.0, 15.3 and 33.8 mg g^{-1} respectively for SSB, SSM, SMB and SMM. The K_L magnitude quantifies the relative affinity between sorbate and sorbent surface. The higher value of K_L observed in the case of SMM compared to SMB and in the case of SSM compared to SSB; demonstrates the superior capacity of cold plasma on sawdust treatment to adsorbed RB2 dye molecules and form stable complexes [54]. The same observation is made with K_g, the Liu constant. The high values of K_f and K_g obtained in the case of SSM compared to SSB on the one hand and in the case of SMM compared to SMB on the other hand indicate that SMM and SSM have a strong affinity for the RB2 dye [45].

Liu is the best match for the adsorption balance of RB2 on raw and treated sawdust. Similar results were obtained by [55]. In addition, the data listed in Table 4 have shown that plasma processing influences the adsorption equilibrium [14]

3.2.7 Kinetic studies

Three kinetic models (Avrami fractional-order, Pseudo-first-order, and Pseudo-second-order) attempted to fit experimental data of RB2 adsorption on sawdust sorbents (SSB, SSM, SMB and SMM) and the results were depicted on Fig. 13. The different kinetic modeling parameters calculated and the correlation coefficients (R^2) are shown in Table 4.

Fig.13: Kinetic adsorption graphs of RB2 onto SSM (a), SSB (b) SMB©, and SMM(d) ($m_{adsorbent}$ SMB, SMM = 0.1 g, ($m_{adsorbent}$SSB, SSM=0.05 T = (293 ± 0.1) K, pH = 1.0 ± 0.1.

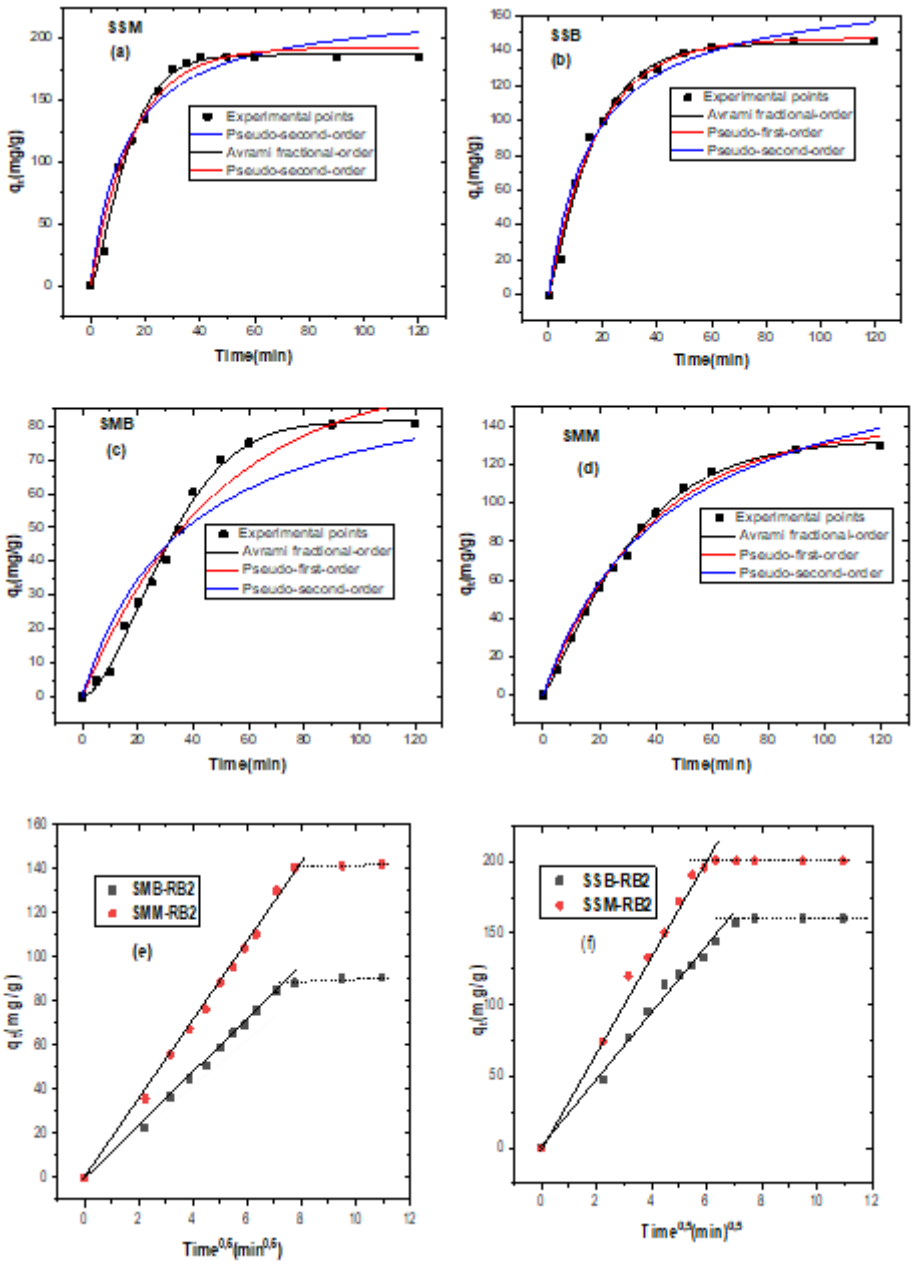

Table 4 Kinetic parameters for RB2 removal using SMB, SMM, SSB and SSM as biosorbents

	SMB	SMM	SSB	SSM
Pseudo-first order				
q_e(mg.g^{-1})	85.52	85.52	146.74	192.72
K_1 (min^{-1})	0.0206	0.0559	0.0555	0.0263
R^2	0.9593	0.9888	0.9888	0.9783
Pseudo-second order				
q_e(mg.g^{-1})	90.52	141.68	176.43	187.78
K_2*10^{-4}(g.mg^{-1}.min^{-1})	2.6561	1.1524	3.5020	3.4027
R^2	0.9086	0.9846	0.9730	0.9448
Avrami				
K_{AV}	0.0285	0.0299	0.0575	0.0665
n_{AV}	1.6796	1.175	1.1330	1.3441
q_e	81.46	133.01	143.78	186.78
R^2	**0.9952**	**0.9998**	**0.9911**	**0.9919**

Conditions: temperature was fixed at 293 K; contact time, pH, and biosorbent dosage were fixed at 90 min, 1.0 and 2.5 g/500mL; 50 min, 1.0 and 2.5g/500mL; 50 min, 1.0 and 1.5 g/ 500 mL; 35 min, 1.0 and 1.5 g/ 500 mL for SMB, SMM, SSB and SSM, respectively

The parameters for each sorbent (SMB, SMM, SSB and SSM) are calculated and gathered for the biosorption of the RR2 dye in Table 4. From the correlation coefficients (R^2), the biosorption on the SMB, SMM, SSB and SSM is best explained by the Avrami-fractional-order kinetics (R^2 = 0, 99) with the RB2 dye. This suggests that the limiting step depends on the physicochemical affinity between the dye and the sorbent surface [57]. Taking into account the initial rate ($h = k_2 qe^2$ for the biosorption taken up by the SMB, SMM, SSB and SSM (table 4), it was observed that this rate (h), on the SMM and the SSM (samples treated with plasma), was higher than those obtained using SMB and SSB (untreated samples) for both dyes. This may be explained by the fact that plasma treatment of Moabi and Sapelli sawdust increases the macrospore (porosity (Fig.6d) and the fibrous appearance (Fig.6b)) on biosorbents due to the acidification of the medium [9, 10], leading to better diffusion of the pollutant, to increased sorption and efficiency of SMM and SSM. Indeed, the plasma when generated in aqueous solution induces a flow of reactive species like radical NO° which enters a series of reactions leading to nitrides and nitric acid via NO_2 and therefore subjected to acidification [46].

3.2.8 Thermodynamic studies

The effect of temperature (303, 313, 323 and 333 K) on the adsorption of reactive blue two (RB2) by sawdust was studied at a fixed amount of adsorbent and at an initial

concentration of RB2 of 50 mg. / L. Portions of 0.1 g of SMB and 0.05 g of SSB were placed in 20 ml vials. The pH of the suspension was adjusted to 1.0. The vials with the contents were stoppered and shaken at 120 rpm in a temperature controlled orbital shaker to improve the reaction equilibrium at room temperature (25 ° C). After 60, 50, 90 and 35 min of processing time for SMB, SMM, SSB and SSM respectively, the suspensions were centrifuged using a centrifuge for 10 minutes at 4000 rpm and the concentration residual of RB2 is determined.

The effect of temperature on the adsorption capacity of SSB, SSM, SMB and SMM at equilibrium time was studied at four different temperatures for a fixed initial concentration of 50 ppm. The amount of RB2 dye adsorbed on the four sawdust samples remained almost constant as the temperatures went from 303 K to 333 K and then decreased with increasing temperature of the solution 333 K. This is mainly due to a decrease in surface activity suggesting that the adsorption of RB2 dye on sawdust was an exothermic process. With increasing temperature, the attractive forces between the wood surface and the anionic dye RB2 are weakened and the tendency of the adsorbate to escape from the adsorbent into solution increases. Similar results have been reported by [29, 43].

The Gibb free energy (ΔG^0), enthalpy (ΔH^0) and entropy (ΔS^0) changes for adsorption of the RB2 dye were determined using Eq. (10) and also from the slope and the interception of a log plot (qe / Ce) compared to 1 / T according to Eq.(11) [43]. The three thermodynamic parameters are presented in Table 5.

Table 5. Thermodynamic parameters for the adsorption of RB2 onto modified and unmodified sawdust

	ΔH^0 (kJ.mol^{-1})	ΔS^0 (kJ.mol^{-1}K^{-1})			ΔG^0 (kJ.mol^{-1})	
Temperature (K)		303	313		323	333
SMB(R=0,95)	-25,35	-0,064	-44,74	-45,38	-46,02	-46,66
SMM(R=0,97)	-35,29	-0,08	-59,53	-60,33	-61,13	-61,93
SSB(R=0,94)	-29,54	-0,068	-50,14	-50,82	-51,50	- 52 ,18
SSM(R=0,98)	-41,16	-0,10	-71,46	-72,46	-73,46	-74,46

Negative values of ΔG^0 showed spontaneous physical adsorption of RB2 on sawdust indicating that this system did not gain energy from an external resource [43, 58]. The decrease in ΔG^0 with increasing temperature indicates that adsorption is more efficient at higher temperature. The enthalpy changes ΔH^0 and the entropy change ΔS^0 for all four samples were negative, suggesting the exothermic nature of the process and

the decrease in randomness at the solid / liquid interface [59]. Untreated sawdust and plasma treated sawdust exhibited almost the same thermodynamic parameters with little improvement in SMM and SSM.

4 CONCLUSION

The wood sawdust of Moabi (Baillonellatoxisperma) and Sapelli (Entandrophragmacylindricum) have been chemically modified by a sliding arc plasma. Sawdust from Moabi and Sapelli in natural form (SMB and SSB) and treated with non-thermal plasma (SMM and SSM) are good alternative absorbents to remove the dye RB2 in aqueous solutions. SMB, SMM, SSB and SSM have been characterized by FTIR spectroscopy, SEM, and TGA/DTG analysis, DRX, chemical analysis by Flouorescence, sorption analyzer and Zetametry. X-ray and elemental analyses also showed that plasma treatment removes impurities and improves the crystallinity of the original wood. The efficiency of the biosorption was strongly dependent on the pH and the contact time. Therefore, the minimum equilibration time with RB2 dye was obtained after 90 min, 50 min and 35 min. From this we made kinetics to explain the biosorption, the Avrami-fractional-order kinetic model provided the best fit. The equilibrium isothermal data were best described by a combination of the Liu isothermal models. Modifications of SMB and SSB increased the biosorption capacity of the dye RB2. The adsorption of the dye RB2 by sawdust from raw Moabi and Sapelli sawdust treated by non-thermal plasma is a spontaneous physical adsorption and the nature of the process is exothermic. The experimental results of the present study reveal that Moabi and Sapelli sawdust are efficient and inexpensive absorbents for the removal of the dye RB2 from the aqueous solution.

ACKNOWLEDGMENTS

Materials and Transformation Unit (UMET), Polymer Systems Engineering UMR CNRS No, 8207, C6 Building, Lille-Sciences and Technology University, 59655 Villeneuve D'Ascq Cedex, France.

Institute of Condensed Matter and Nanosciences (IMCN), Division Molecular Chemistry, Materials and Catalysis (MOST), UCLouvain, Place Louis Pasteur 1, box L4.01. 09, B-1348 Louvain-la-Neuve, Belgium.

Abraham Bin NGONGO, may God be your reward for the support and may he bless you richly.

Professors Elie Acayanka and Jean-Baptiste TARKWA, thank you for your input.

REFERENCES

[1] H.-Z.Li, Y.-N. Zhang, J.-Z. Guo, J.-Q. Lv, W.-W. Huan, B.Li. Preparation of hydrochar with high adsorption performance for methylene blue by co-hydrothermal carbonization of polyvinyl chloride and bamboo. Biores. Technol. 337 (2021) 125442.

[2] M.L.De Sousa, P.B.De Moraes, P.R.M Lopes, R.N.Montagnolli, D.F.De Angelis, E.D.Bidoie Contamination by Remazol Red Brilliant dye and its impact in aquatic photosynthetic microbiota. Environ Manag Sustain Dev (2012) 1(2):129–138.

[3].P.S.Ratna, Padhi PS Pollution due to synthetic dyes toxicity & carcinogenicity studies and remediation. Int J Environ Sci 3 (3) (2012) : 940– 955.

[4] T. N. Viera de Souza, D. do Socorro, B. Brasil. Adsorption of Basic dyes onto activated carbon : Experimental and theoritical investigation of chemical reactivity of basic dyes using DFT-based descriptors Appl. Surf. Sci. 448 (2018) 662-670.

[5] L. C. Peterle do Nascimento, A. M. Miranda da Costa, A. R.da Silva, A. V. Nardy Ribeiro, J. Nardy Ribeiro. Banana peel powder and sawdust powder for methylene blue removal in water, Braz. J. Dev. 8 (4) (2022) 32253-32277.

[6] S.S. moghaddam, M.R.A. Moghaddam, M. Arani. Coagulation/floculation process for dye removal using sludge from water treatment plant : optimization through response surface methodology J. Hazard. Mater 175(1-3) (2010) : 651-657.

[7] C. Bhattacharjee, S. Dutta, V.K. Saxena, A Review on biosorptive removal of dyes and heavy metals from waste water using watermelon ring as biosorbent. Environ. Adv.2 (2020) 100007.

[8] B. Takam, E. Acayanka, G.Y. Kamgang, M.T. Pedekwang, S. Laminsi., Enhancement of sorption capacity of cocoa shell biomass modified with non-thermal plasma for removal of both cationic and anionic dyes from aqueous solution, Environ. Sci. Pollut. Res. (2017) 24:16958–16970.

[9] L.D.T Prola, E. Acayanka, E.C. Lima, C.S. Umpierres, C.P. Julio, Vaghetti, O.S. Wmekson, S. Laminsi, P.T. Djifon. Comparison of Jatrophacurcas shells in natural form and treated by non-thermal plasma as biosorbents for removal of Reactive Red 120 textile dye from aqueous solution. *Ind Crop Prod* (2013) *46:328–340.*

[10] A. N. Alene , G. Y. Abate, A. T. Habte, Bioadsorption of Basic Blue Dye from Aqueous Solution onto Raw and Modified Waste Ash as Economical Alternative Bioadsorbent. J.Chem. (2020) 11 pp

[11] J.R.Ngueguim., L.Zapfack, J.G.Makombu., Foahom, B., 2009. Le Moabi (B. toxis perma) un arbre multi-ressources des forêts denses humide du Cameroun. Le Flamboyant 65, 2–5.

[12] M. Lourmas, F.Kjellberg, H.Dessard, H.I.Joly, M.H.Chevallier (2007) Reduced density due to logging and its consequences on mat ing system and pollen flow in the African mahogany Entandro phragma cylindricum. Heredity 99(2) :151–160.

[13] A.Kesraoui, A. Moussa, G. B. Ali, M. Seffen. Biosorption of alpacide blue from aqueous solution by lignocellulosic biomass: Luffa cylindrica fibers. Environ Sci Pollut Res 23 (2016) 15832–15840.

[14] F. Banisheykholeslami, M.Hosseini, G.N. Darz. Design of PAMAM grafted chitosan dendrimers biosorbent for removal of anionic dyes: Adsorption isotherms, kinetics and thermodynamics studies, Int. J. Biol. Macromol. 177 (2021) : 306–316.

[15] I. Akkari · Z. Graba · Nacer Bezzi · F. Ait Merzeg · N. Bait · A. Ferhati. Raw pomegranate peel as promise efficient biosorbent for the removal of Basic Red 46 dye: equilibrium, kinetic, and thermodynamic studies. Biomass Convers. Refin. (2021) 14 pp.

[16] C.P. Nanseu-Njiki, G KenneDedzo, E. Ngameni. Study of the removal of paraquat from aqueous solution by biosorption onto Ayous (Triplochitonschleroxylon) sawdust. J Hazard Mater. 179 (2010): 63–71.

[17] H. Patnukao, P. Pavasant, Activated carbon from Eucalyptus camaldulensis Dehn bark using phosphoric acid activation, Bioresour.Technol.99(2008) 8540-8543.

[18] M.E.M. Ali, A.M. Abd El-Aty, M.I. Badawy, R.K. Ali. Removal of pharmaceutical pollutants from synthetic wastewater using chemically modified biomass of green alga Scenedesmus obliquus. Ecotoxicol. Environ. Saf. 151 (2018) 144–152.

[19] K. Benabbas, N. Zabat, I. Hocini. Study of the chemical pretreatment of a nonconventional low-cost biosorbent (Callitriche obtusangula) for removing an anionic dye from aqueous solution. Euro-Mediterr. J. Environ. Integr. 6 :54 (2021) 17pp

[20] M.A. Martin-Lara, G. Biosorbents To Remove Heavy Metal from Aqueous Solutions by Chemical Treatment of Olive Stone, Ind.Chem.Res.52(2013) 10809-10819.

[21] V.K Hem Lata, R. K Garg, Removal of a basic dye from aqueous solution by adsorption using Parthenium hysterophorus: An agricultural Waste Dyes Pigments 74(2007) 653-658

[22] W. Zou, H. Bai, S.Gao; K. Li; characterization of modified sawdust kinetic and equilibrium study about methylene blue adsorption in batch mode , K J.Chem. Eng.30 (1) (2013)111-122.

[23] S ;Laminsi, E .Acayanka, S.Nzali, P.T.Ndifon, J.L.Brisset Direct impact and delayed post-discharge chemical reactions of Fe(II) complexes induced by non-thermal plasma. Desal Water Treat (2012) 37:38–4.

[24] J.L. Brisset, D.Moussa, A.Doubla, E.Hnatiuc, B.Hnatiuc, Y.G.Kamgang, J.M.Herry, .Naitali, Bellon-Fontaine MN Chemical reactivity of discharges and temporal post-discharges in plasma treatment of aqueous media: examples of gliding arc discharge treated solutions. Ind Eng Chem Res (2008) 47:5761–5781.

[25] T. Wang, J. Liu, Y. Zhang, H. Zhang, W-Y. Chen, P. Norris, W-P. Pan, Use of a non-thermal plasma technique to increase the number of chlorine active sites on biochar for improved mercury removal, Chem. Eng. J (2018) 536-544.

[26] H.A. Al-Yousef, B.M. Alotaibi, M.M. Alanazi, F. Aouaini, L. Sellaoui, A. Bonilla-Petriciolet. Theoretical assessment of the adsorption mechanism of ibuprofen, ampicillin, orange G and malachite green on a biomass functionalized with plasma. J. Environ. Chem. Eng. 9 (2021).

[27] Z. Košelová , J. Ráhel', O. Galmiz. Plasma Treatment of Thermally Modified and Unmodified Norway Spruce Wood by Diffuse Coplanar Surface Barrier Discharge. Coatings 2021, 11, 40.

[28] S. Kodama, H.Habaki, H.Skiguchi, Kawasaki, Surface modification of adsorbent by dielectrc barrier discgarge, Thin Solid Films 407(2002) 151-155.

[29] A. Tursi, N. De Vietro, A. Beneduci, A. Milella, F. Chidichimo, F. Fracassi, G. Chidichimo, Low pressure plasma functionalized cellulose fiber for the remediation of petroleum hydrocarbons polluted water, J. Hazard. Mater. 373 (2019), 773-7827.

[30] F.L. Digabel, L. Avérous, Effects of lignins content on the properties of lignocellulosebased biocomposites, Carbohyd. Polym., 66, (2006). 537-545.

[31] S. Benyoucef, Dj. Harrache. Microstructure characterization of Scot pine "Pinus Sylvestris" sawdust Mater. Environ. Sci. 6 (3) (2015) 765-772.

[32] A. Czernichowski GlidArc assisted preparation of the synthesis gas from natural and waste hydrocarbons gases. Oil Gas Sci. Technol. Rev. IFP 56: (2001) 181–198.

[33] L. Mooktzeng, A.Z.Zulkifli-shah. Investigation of biomass surface modification using non- plasma. Plasma science and technology 20(11), (2018)115502**.**

[34] Zhang, Y. Duana†, Q. Zhou, C. Zhu, M. Shea, W. Ding, Adsorptive removal of gas-phase mercury by oxygen non-thermal plasma modified activated carbon. Chem. Eng. J 294 (2016) 281-289.

[35] E. Nithya, R. Radhai, R. Rajendran, S. Shalini, V. Rajendran, S. Jayakumar Synergetic effect of DC air plasma and cellulase enzyme treatment on the hydrophilicity of cotton fabric. CarbohydrPolym(2011) 83:1652–1658.

[36] M. Simo-Tagne, R. Rémond, Y. Rogaume, A. Zoulalian., P. Perré, characterization of sorption behavior and mass transfer properties of four central africa tropical woods: ayous, sapele, frake, lotofa, *Maderas.* Ciencia y tecnología 18(1): (2016)207 - 226,

[37] C.C. Da Silva, A. De Faria Lima, J.A. Moreto, S. Dantas, M.A. Henrique, D Pasquini, E.C. Rangel, J. Scarmínio, RV. Gelamo, Influence of plasma treatment on the physical and chemical properties of sisal fibers and environmental application in adsorption of methylene blue. Mater. Today Commun. 23 (2020) 101140.

[38] Z.M. Magriotis, M.Z. Carvalho, P.F. de Sales, F.C. Alves, R.F. Resende, A.A. Saczk. Castor bean (Ricinuscommunis L.) presscake from biodiesel production: an efficient low cost adsorbent for removal of textile dyes. J Environ Chem Eng. (2014); 2:1731–1740.

[39] J. Morales, M. G. Olayo, G. J Cruz, P.Herrera-Franco, R. Olayo., Plasma Modification of Cellulose Fibers for Composite Materials, Journal of Applied Polymer Science, Vol. 101, (2006) 3821–3828.

[40] D.L. Sun, R.Y. Hong, F. Wang, J.Y. Liu, M.R. Kumar. Synthesis and modification of carbon nanomaterials via AC arc and dielectric barrier discharge plasma. Chem. EngJ(2016) 28:9-20.

[41] Chesseu M.D., Acayanka E., Takam B., Leundjeu N. L, Kamgang Y.G., Laminsi S., Sellaoui L., Bonilla-Petriciolet, Influence of plasma-based surface functionalization of palm fibers on the adsorption of diclorofenac from water: experimenst, thermodynamics and removal mechanism. J. Water Process. Eng. 43(2021) 102254.

[42] C.Saucier, M.A.Adebayo, E.C.Lima, R.Cataluna, P.S.Thue, L.D.T Prola, M.J. PuchanaRosero, F.M Machado, F.A.Pavan, Dotto GL Microwave-assisted activated carbon from cocoa shell as adsorbent for removal of sodium diclofenac and nimesulide from aqueous effluents. J. Hazard. Mater. (2015) 289: 18–27.

[43] S.S. Vieira, Z.M. Magriotis, N.A.V. Santos, M .dG. Cardoso, A.A. Saczk. Macauba palm (Acrocomiaaculeata) cake from biodiesel processing: an efficient and low cost substrate for the adsorption of dyes. Chem. Eng. J. 183 (2012): 152–161.

[44] B.H. Hameed, A.A. Ahmad. Batch adsorption of methylene blue from aqueous solution by garlic peel, an agricultural waste biomass. J. Hazard. Mater. 164 (2009): 870–875.

[45] D.Sedan, C.Pagnoux, A.Smith, T.Chotard Interaction fibre de chanvre/ciment: influence sur les propriétés mécaniques du composite. Mater Tech (2007) 5:133-142.

[46] C.C. Da Silva, A. De Faria Lima, J.A. Moreto, S. Dantas, M.A. Henrique, D Pasquini, E.C. Rangel, J. Scarmínio, RV. Gelamo, Influence of plasma treatment on the physical and chemical properties of sisal fibers and environmental application in adsorption of methylene blue. Mater. Today Commun. 23 (2020) 101140.

[47] A. Leal Vieira Cubas, M. Medeiros Machado, R.Tayane Bianchet, K. A. da Costa Hermann, J. Al. Bork, N. A. Debacher, E. F. Lins, M. Maraschin, D. Sousa Coelho, E.H. Siegel Moecke. Oil extraction from spent coffee grounds assisted by non-thermal plasma Sep. Purif. Technol. 250 (2020) 117171.

[48] T. Felix. J.S. Trigueiro, N. Bundaleski, O.M.N.D. Teodoro, S. Sério., N.A. Debacher. Functionalization of polymer surfaces by medium frequency non-thermal plasma, Appl. Surface Science (2017).

[49] J.Y. Kanmogne., A. Talla., A., L. Monkam. Experimental Determination and Modelling of Water Desorption Isotherms of Tropical Woods: Afzelia, Ebony, Iroko, Moabi and Obeche. HolzalsRoh-und Werkstoff 64(2) (2006): 121 - 124.

[50] V. K. Garg, R. Gupta, A. B. Yadav, and R. Kumar, “Dye removal from aqueous solution by adsorption on treated sawdust. Bioresource Technology 89(2) (2003). pp. 121–124.

[51] W. Cui , Y. Xu, G. Luo, Q. Zhang, Z.. Li, S. Zhang. Enhanced mercury removal performance of Cu-Fe binary oxide sorbents modified by non-thermal plasma. Chem. Eng. J. 425 (2021) 131851

[52] G-Z. Qu, J. Li, D.-L. Liang, D.-L. Huang, D. Qu, Y.-M. Huang. Surface modification of a granular activated carbon by dielectric barrier discharge plasma and its effects on pentachlorophenol adsorption. J. Electrostat. 71 (2013) 689-694.

[53] M. Shi, G. Luo, Y. Xu, R. Zou, H. Zhu, J. Hu, X. Li, H.Ya. Using H_2S plasma to modify activated carbon for elemental mercury removal. Fuel 254 (2019) 115549

[54] S.Dawood, T.K. Sen Removal of anionic dye Congo red from aqueous solution by raw pine and acid-treated pine cone powder as adsorbent: equilibrium, thermodynamic, kinetics, mechanism and process design. Water Res 46 (2012) 1933–1946.

[55] M. Kaur, M. Datta. Adsorption be haviour of reactive red 2 (RR2) textile dye onto clays: equilibrium and kinetic studies. Eur. Chem. Bull. 3(8)(2014) 838–849.

[56] B. Takam ,J-B. Tarkwa, E. Acayanka, S. Nzali, M.D. Chesseu , Y.G. Kamgang, S. Laminsi. Insight into the removal process mechanism of pharmaceutical compounds and dyes on plasma-modified biomass: the key role of adsorbate specificity. Environ. Sci. Pollut Res. 27 (2020) 20500–20515.

[57] M. Antunes, V.I. Esteves, R. Guégan, J.S. Crespo, A.N. Fernandes, M. Giovanela.Removal of diclofenac sodium from aqueous solution by Isabel grape bagasse. J. Eng. Chem. 192 (2012) 114–121.

[58] V. Vimonses, S. Lei, B. Jin, C.W.K., Chow, Saint, C.,.Kinetic study and equilibrium isotherm analysis of Congo red adsorption by clay materials. Chem. Eng. J. 148 (2009) 354–364.